Visualizations of Liquid Breakup by Fuel Slingers

Werner J.A. Dahm[1], Prashant R. Patel[2], Bryan H. Lerg[3]

1. Professor of Aerospace Engineering and Head, Laboratory for Turbulence & Combustion (LTC), Department of Aerospace Engineering, The University of Michigan, Ann Arbor, MI 48109-2140, USA.
2. Undergraduate Student, Department of Aerospace Engineering, The University of Michigan, Ann Arbor, MI 48109-2140, USA.
3. Graduate Student, Department of Aerospace Engineering, The University of Michigan, Ann Arbor, MI 48109-2140, USA.

Results are shown from experiments on liquid breakup by rotary centrifugal atomizers of the type used in small gas turbine engines. Pulsed laser visualizations reveal the breakup process at various rotation rates for different hole sizes and shapes. Liquid is seen to issue as a film from the entire hole periphery. Key breakup regimes are identified, including subcritical and supercritical modes. Mode transition parameters and breakup characteristics are obtained in terms of design and operating variables.

1. Introduction

Small gas turbines for business jets, standoff munitions, and unmanned aerial vehicles often use rotary centrifugal atomizers for fuel spray formation. Unlike large gas turbine engines, where the fuel is pressure-atomized by a high-pressure fuel pump, as the engine dimensions are reduced the fuel pump does not scale in size or weight with the rest of the engine, and pressure atomization becomes increasingly disadvantageous. The high rotation rates at which small gas turbines operate allow rotary centrifugal atomizers to provide the fuel spray. Rotary atomizers are widely used in many different spray processes [1, 2]; the type used in turbine engines is referred to as a *fuel slinger*. While slingers have been used in small gas turbine engines [3, 4] as well as certain other combustion applications for over 30 years, their development has to date been largely empirical. Since slinger atomization performance plays an important role in the turbine engine operation, there are strong incentives for placing the design of such slingers and the understanding of their performance characteristics on an improved foundation. The present study provides flow visualizations of the liquid breakup process in fuel slingers over a range of hole geometries, hole sizes, and slinger rotation rates. The results are used to identify fundamental physical processes and scalings relevant to liquid atomization by fuel slingers.

2. Slinger design and operating parameters

The generic fuel slingers considered here consist of an axisymmetric disc rotating at a rate Ω with N identical channels located in a rim at the edge of the disc and oriented along the radial direction. Liquid is supplied to the disc face at total volume flow rate Q, giving $q \equiv Q/N$ as the

volume flow rate per channel. The channels may be holes with diameter d, or any other shape that produces desirable atomization performance. The channel entrance and exit are located at radii R_1 and R_2, with the channel length $L \equiv (R_2 - R_1)$. In practice, $L \ll R_2$ and thus the nominal radius is $R \equiv {}^1/_2(R_1+R_2)$. For a given hole shape, the slinger geometry and hole characteristics primarily affect the nominal liquid film thickness t and the bulk film velocity U_b in the channels. From [5] these are given by

$$t = \left[\frac{3}{\quad} \right]^{1/3} \left[\frac{\rho_L q}{\rho_L R \Omega^2 d} \right]^{1/3} \quad \text{and} \quad U_b = \frac{q}{\Omega d t} \quad . \qquad (1a,b)$$

For circular holes, atomization performance thus depends on the film thickness t, the channel diameter d, and the crossflow velocity $U_c \equiv R\Omega$ into which the film issues, together with the liquid and gas properties. The resulting governing dimensionless parameters are the corresponding Weber and Ohnesorge numbers

$$We \equiv \left[\frac{\rho_G U_c^2 t}{\sigma_L} \right] \quad \text{and} \quad Oh \equiv \left[\frac{\mu_L}{(\rho_L \sigma_L t)^{1/2}} \right] \quad , \qquad (2a,b)$$

together with the liquid-gas density ratio $r \equiv [\rho_L/\rho_G]$, the liquid-gas viscosity ratio $m \equiv [\mu_L/\mu_G]$, and the relative film thickness $s \equiv [t/d]$. It was noted in [5] that fuel slingers typically operate at conditions for which the effects of r, m and Oh on atomization performance are negligible. The resulting drop size distributions thus depend principally on We and s. For noncircular holes, the principal effect of hole shape will be seen below to be a modification of the nominally uniform film thickness due to surface tension effects.

3. Visualizations of liquid breakup in fuel slingers

3.1. Experimental arrangement

Instantaneous visualizations of the liquid break process for various slinger hole geometries over a range of rotation rates were obtained using Nd:YAG laser-based flash photography. Five different slinger hole geometries were considered, as indicated in Fig. 1. Each consisted of a 4-in. diameter disc with a rim containing 16 identical equally-spaced slinger holes. The disc diameter is representative of typical values for slingers used in small gas turbine engines. The slinger rim was flat on both sides, with an inner diameter of 3.75-in. and an outer diameter of

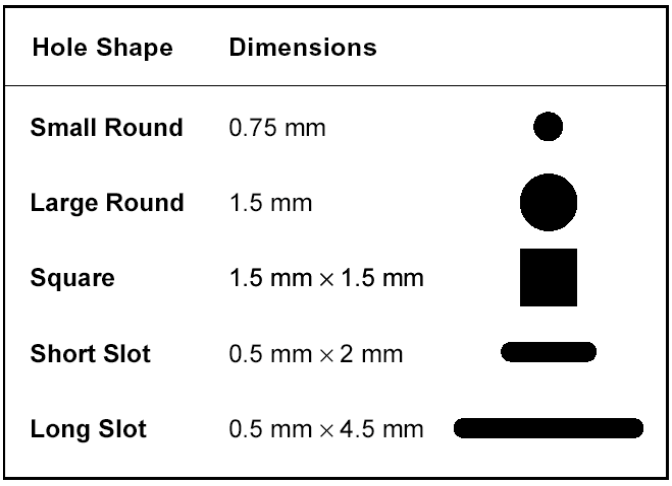

Fig. 1. Hole shapes and dimensions for the five slingers, denoted SR, LR, SQ, SS and LS. The LR and SS holes have the same equivalent diameter.

4.00-in. Channels with the cross-sectional shapes given in Fig. 1 were EDM fabricated with very fine tolerance straight through this rim, producing 0.125-in. long channels through which the liquid flowed from the disc to issue from each of the slinger holes. The slingers were driven by a router motor with an electronic controller. Rotation rates ranged from 900 - 17,800 rpm, spanning the representative range of engine relight conditions in small gas turbine engines. Tap water was fed onto the slinger disc via a pump. The liquid flow rate was controlled and measured by an in-line rotameter, and was held constant at 8 gpm, representative of practical fuel flow rates in small gas turbines at these speeds. Visualizations were obtained by indirectly illuminating the liquid breakup process with 532 nm light pulses of 10 nsec duration from a frequency-doubled Nd:YAG laser. A simple 35 mm camera recorded the breakup pattern on standard ISO 100 film using a Vivatar macro lens. For any given hole geometry at any fixed rotation rate, the liquid breakup pattern was observed to be highly repeatable, despite the fact that strikingly different features were seen in the breakup patterns at different rotation rates and for different hole geometries.

3.2. Experimental results

Figs. 2-6 show the liquid breakup for each slinger hole shape over a range of rotation rates. These show clear trends in the breakup patterns and drop sizes as *We* increases with rotation rate. Significant differences are also apparent at the same rotation rate among the various hole shapes. Figs. 7 and 8 show enlarged views of several key phemomena. It is apparent at many of these conditions that the fluid emerges from the channels in a thin film around the entire periphery of the hole. The cumulative effect of Coriolis forces on the film flow along the channel walls is apparently not sufficient to accumulate the fluid on one side of the channels; this is discussed in greater detail in [5]. It is also apparent in these visualizations that the film issuing from the channel exit can either directly break up as a thin liquid sheet, or can form into a ligament and subsequently undergo Rayleigh-type liquid column breakup. The conditions for which the crossover between these two modes of operation occurs are discussed in §4.2. Moreover, it is seen in the square-hole and the two slot-hole results that these shapes can lead to ligaments issuing from those parts of the channel where the radius of curvature is high; this is discussed in §4.3. It is also seen at low rotation rates that, while the liquid film issues from the entire hole periphery, it can flow *along* the slinger face *away* from the hole and accumulate on the face near the hole. Centrifugal forces subsequently cause the resulting liquid pool to form irregular ligaments which then undergo ligamentary breakup. The irregular nature of the resulting ligament formation leads to larger variance in the drop size distribution. This is most pronounced for the square hole slinger, and may be connected with the higher surface tension effect in the four corners. Such irregular breakup is considered in §4.4.

4. Liquid breakup transition parameters

4.1. Coriolis effects on film formation

In [5] it was shown that the effect of radial forces on the film flow in the channels is small enough for typical slinger design and operating parameters that the liquid issues from the entire periphery of the channel as a film. This is confirmed by the visualizations in Figs. 2-8. Under such conditions the slinger operates in *film mode*, and subsequent liquid breakup is dominated by the film thickness *t*. However if Coriolis effects are sufficient to accumulate the liquid in a single stream on one side of the channel, then the slinger operates in *stream mode*, and subsequent breakup is dominated by the stream diameter *d*. The resulting stream

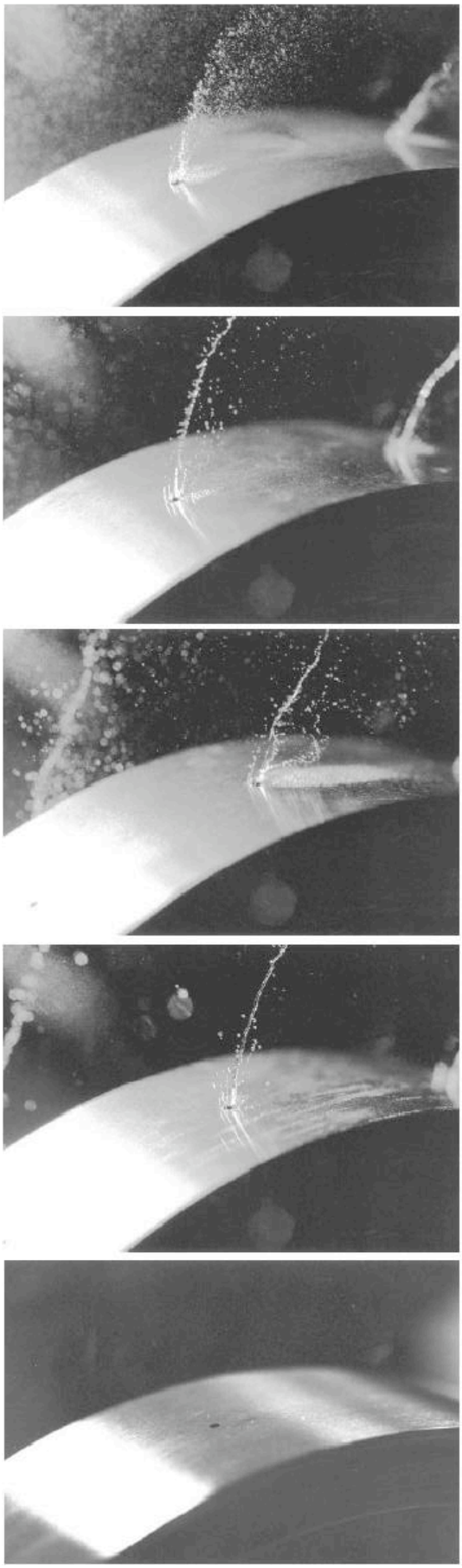

Fig. 2. Small round hole (SR) slingers at 4300, 7800, 9500, and 17,800 rpm *(top)*.

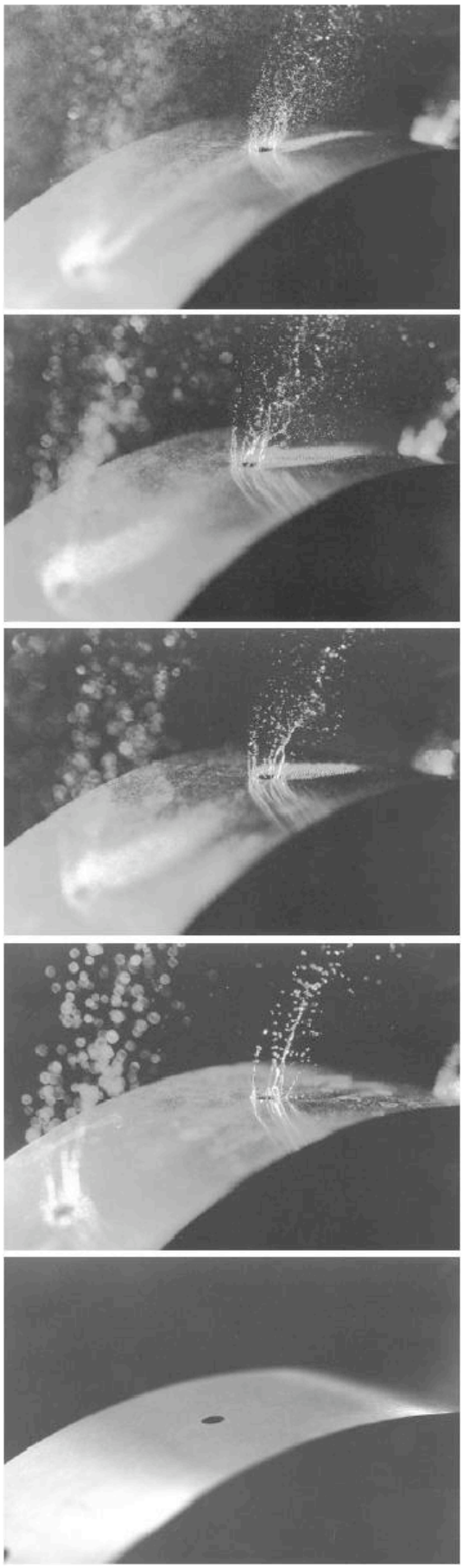

Fig. 3. Large round hole (LR) slingers at 4300, 7800, 9500, and 17,800 rpm *(top)*.

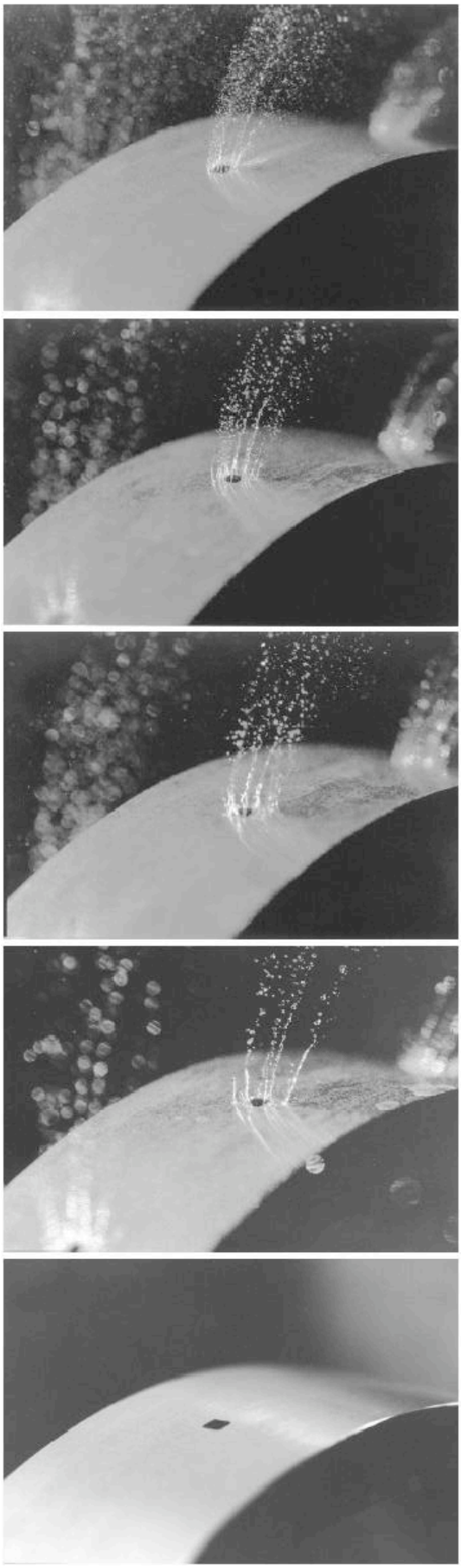

Fig. 4. Square hole (SQ) slingers at 4300, 7800, 9500, and 17,800 rpm *(top)*.

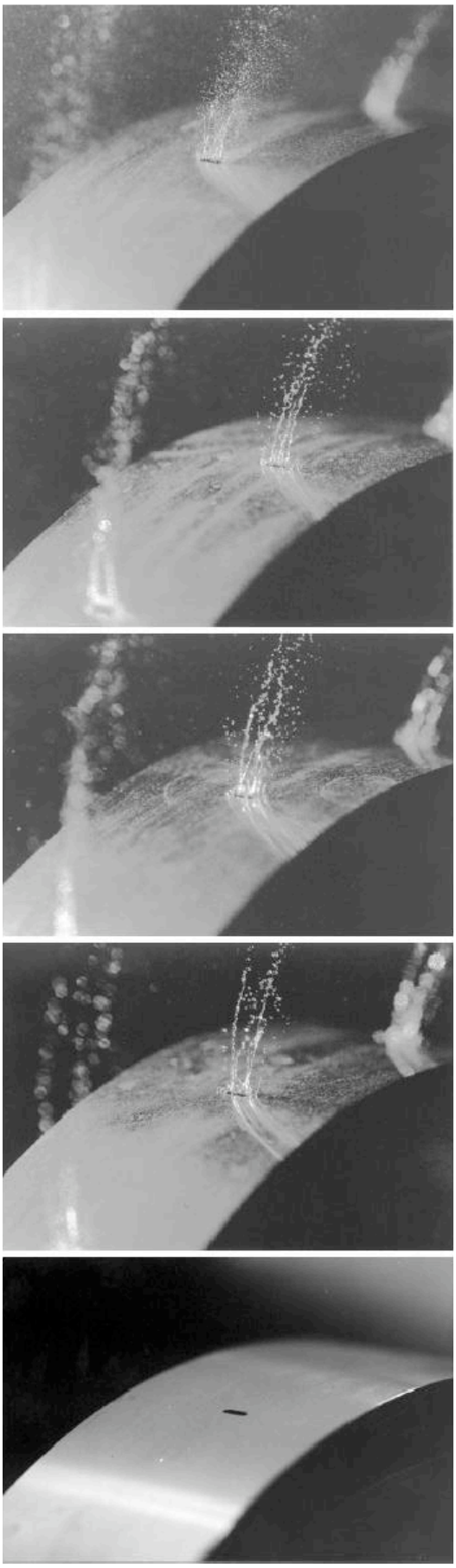

Fig. 5. Short slot (SS) slingers at 4300, 7800, 9500, and 17,800 rpm *(top)*.

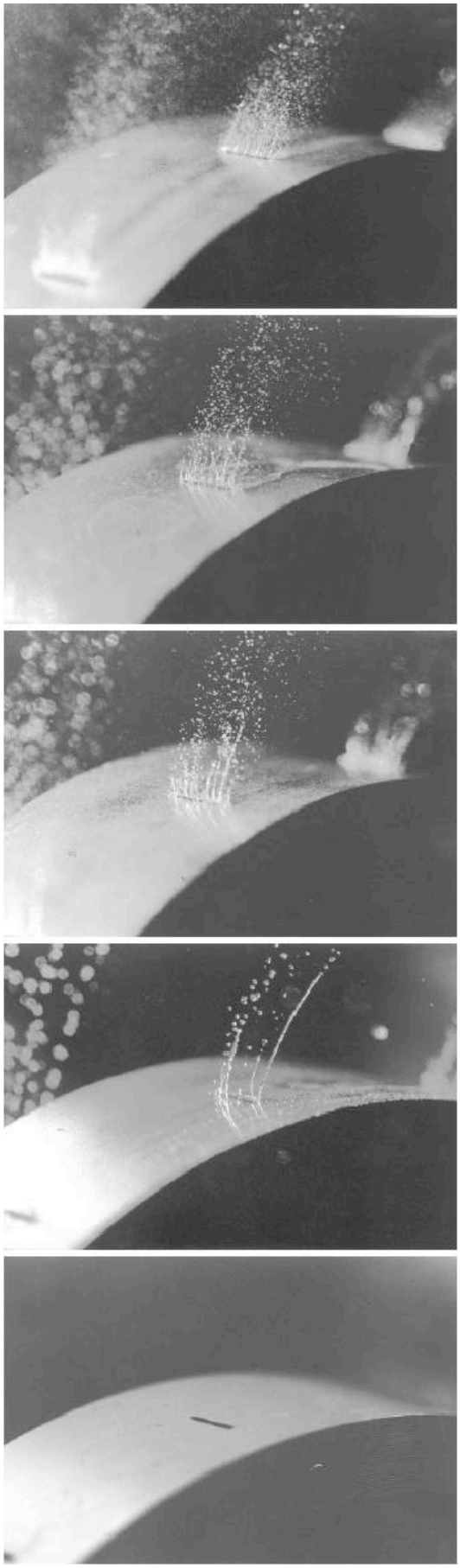

Fig. 6. Long slot (LS) slingers at 4300, 7800 9500, and 17,800 rpm *(top)*.

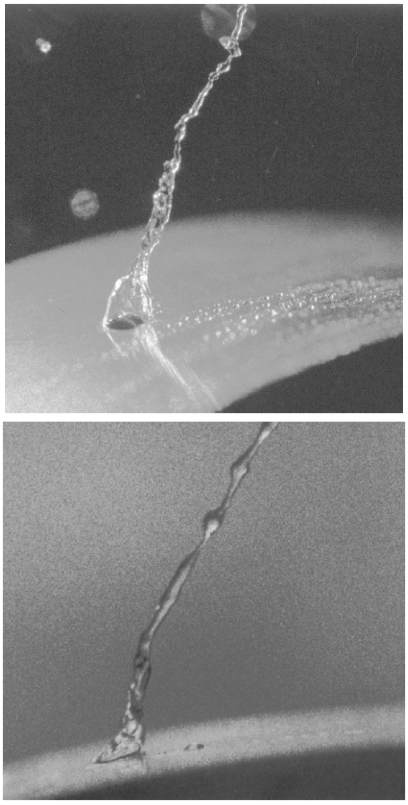

Fig. 7. Oblique and side views of subcritical film breakup on the LR slinger at relatively low rotation rates.

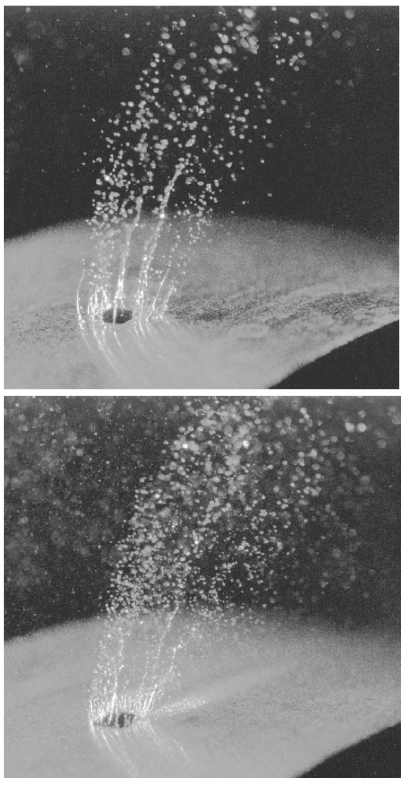

Fig. 8. Irregular *(top)* and regular *(bottom)* film mode breakup on the SQ slinger at 9,500 and 17,800 rpm .

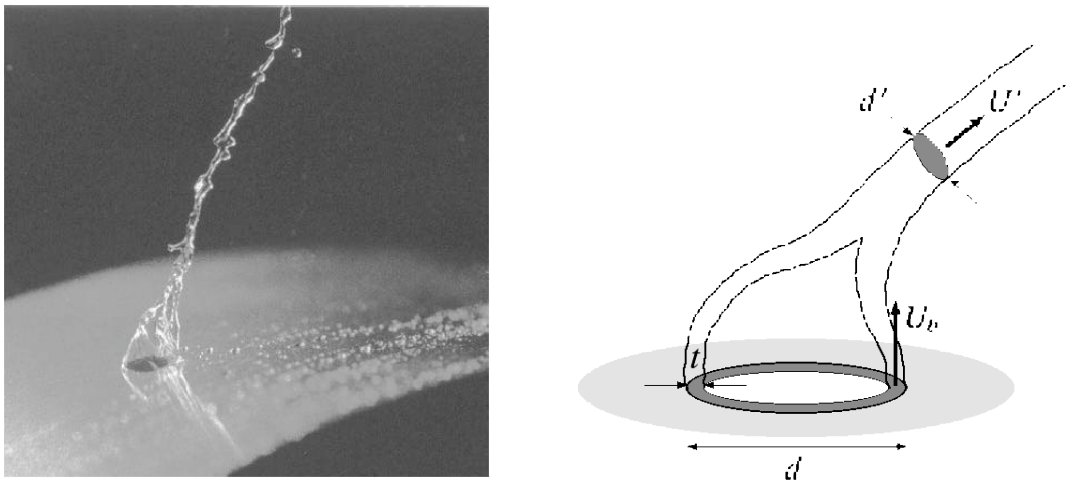

Fig. 9. Subcritical film mode breakup; initial liquid film with thickness t issuing at bulk velocity U_b along periphery of channel with diameter d is collapsed by surface tension into a single ligament with diameter d_* and bulk velocity U_* given by (5*a,b*).

characteristics can be determined in a similar manner as discussed in §4.2. The condition for which Coriolis effects transition the slinger from film mode to stream mode was given in [5].

4.2. Subcritical vs. supercritical film breakup

The visualizations in Figs. 2-6 confirm that the liquid nominally issues from the entire periphery of the channel in a liquid film, with thickness t and bulk velocity U_b given by (1*a,b*). Upon issuing from the channel exit, surface tension acts to collapse the film together toward its center. The time scale τ for this collapse, as well as the bulk advective time scale (d/U_b) with which the film issues from the channel, are given by

$$\tau \sim \left(\frac{\rho_L d^2 t}{\sigma_L} \right)^{1/2} \quad \text{and} \quad (d / U_b) \sim \left(\frac{d^2 t}{q} \right) \qquad (3a,b)$$

If τ is sufficiently small relative to (d/U_b) then surface tension will succeed in collapsing the film into a single ligament having diameter d_* and bulk velocity U_* as indicated in Fig. 7. The resulting ligament will undergo Rayleigh breakup to produce drop sizes of $O(d_*)$; this is termed *subcritical breakup*. If however τ is sufficiently large compared to (d/U_b) then the film survives and breaks up to produce drop sizes of $O(t)$; this is termed *supercritical breakup*. The time scale ratio gives the transition parameter between subcritical and supercritical breakup as

$$S \equiv \left(\frac{q^2 \rho_L}{d^2 t \sigma_L} \right)^{1/2} \quad . \qquad (4)$$

For small S, the resulting subcritical ligament having diameter d_* and bulk velocity U_* in Fig. 9 are obtained by matching the mass flux $M \equiv \rho_L q$ and momentum flux $J \equiv \rho_L U_b^2 \pi d t$ of the film flow issuing from the channel, giving

$$d_* = \frac{2M}{(\pi \rho_L J)^{1/2}} \quad \text{and} \quad U_* = \frac{J}{M} \quad . \qquad (5a,b)$$

At low rotation rates, a slinger that otherwise operates in supercritical film mode ($S > S_{critical}$) can transition to subcritical mode, leading to correspondingly larger drop sizes.

4.3. Effect of noncircular channels

The high surface tension produced by the small radius of curvature at each concave corner in a noncircular channel can accumulate the liquid film initially flowing along the channel walls of a film mode slinger into concentrated ligaments [5]. The number n of such ligaments depends on the channel shape. Evidence of such corner ligaments can be seen on the SS, LS, and SQ slingers in Figs. 2-6. Since the surface tension effect is cumulative, the extent of liquid accumulation into such corner ligaments increases with channel length L and decreases with decreasing film thickness t. The remaining liquid issues in a film from the channel periphery. If all of the liquid accumulates in the ligaments, then the resulting ligament diameter d_{ℓ} and bulk velocity U_{ℓ} can again be found by matching the mass and momentum flux of the initial film flow with that of the ligaments. The mass and momentum fluxes are then on a *per ligament* basis; thus for example M and J above are replaced by M/n and J/n if all corners are identical.

4.4. Regular vs. irregular film mode breakup

Fig. 8 shows the transition from *irregular* to *regular* film mode breakup. In the former, the thin liquid film issuing from the periphery of the hole does not leave the slinger face, and instead flows along the face away from the hole, presumably due to surface tension. The resulting liquid pool then forms into ligaments leaving the slinger face that subsequently undergo ligamentary breakup. The process by which this irregular mode occurs is not well understood, but the phenomenon appears to be confined to relatively low rotation rates and is most pronounced for hole shapes having small radii of curvature [5].

5. Conclusions

Visualizations of liquid breakup by generic fuel slingers have identified fundamental processes that provide the basis for relating the drop size distributions to slinger design and operating parameters. Fundamental considerations of the flow within the channels, including Coriolis effects and surface tension effects, suggest that slingers operate in either a *film mode* with drop sizes of $O(t)$ or a *stream mode* with drop sizes of $O(d_{\ell})$. Effects of fluid properties and various slinger design and operating parameters on the transition between these modes have been identified. Further consideration of surface tension effects on the film issuing from the periphery of the channels has identified *subcritical* and *supercritical* regimes for film mode breakup. In addition, *irregular* breakup occurring at low rotation rates for hole shapes with sharp corners leads to large variance in drop sizes. Noncircular channels serve only to produce stronger concave curvature in the film, which can lead to ligament formation and correspondingly larger drop sizes. Based on these considerations, the finest drop sizes should be expected from slingers having a relatively thin rim with a comparatively large number of large-diameter circular channels operating at supercritical values of the transition parameter S. Resulting drop sizes should then be of the order of the film thickness t in (1*a*).

6. References

[1] Lefebvre, A 1989 *Atomization and sprays* (Washington: Taylor & Francis).
[2] Bayvel, L and Orzechowski, Z 1993 *Liquid atomization* (Washington: Taylor & Francis).
[3] Rogo, C and Trauth, RL 1974 *SAE Paper 74-0167* (New York: SAE).
[4] Morishita, T 1981 *ASME Paper 81-GT-180* (New York: ASME).
[5] Dahm, WJA, Patel, PR and Lerg, BH 2002 *AIAA Paper 2002-3183* (Washington: AIAA).